International Journal of Applied Earth Observation and Geoinformation 33 (2014) 255–269

Contents lists available at ScienceDirect

International Journal of Applied Earth Observation and Geoinformation

journal homepage: www.elsevier.com/locate/jag

Geologic remote sensing for geothermal exploration: A review

Freek van der Meer[a,*], Christoph Hecker[a], Frank van Ruitenbeek[a], Harald van der Werff[a], Charlotte de Wijkerslooth[b], Carolina Wechsler[b]

[a] University of Twente, Faculty of Geo-information Science and Earth Observation (ITC), Hengelosestraat 99, 7514 AE Enschede, The Netherlands
[b] Transmark Renewables, Herengracht 386, 1016 CJ Amsterdam, The Netherlands

ARTICLE INFO

Article history:
Received 9 January 2014
Accepted 21 May 2014
Available online 29 June 2014

Keywords:
Geothermal exploration
Alteration mineralogy
Temperature
Heat flux
TIR/SWIR remote sensing
Pacana geothermal system (Chili)

ABSTRACT

This paper is a comprehensive review of the potential for remote sensing in exploring for geothermal resources. Temperature gradients in the earth crust are typically 25–30 °C per kilometer depth, however in active volcanic areas situated in subduction or rift zones gradients of up to 150 °C per kilometer depth can be reached. In such volcanic areas, meteoric water in permeable and porous rocks is heated and hot water is trapped to form a geothermal reservoir. At the Earth's surface hot springs and fumaroles are evidence of hot geothermal water. In low enthalpy systems the heat can be used for heating/cooling and drying while in high enthalpy systems energy is generated using hot water or steam. In this paper we review the potential of remote sensing in the exploration for geothermal resources. We embark from the traditional suite of geophysical and geochemical prospecting techniques to arrive at parameters at the Earth surface that can be measured by earth observing satellites. Next, we summarize direct and indirect detection of geothermal potential using alteration mineralogy, temperature anomalies and heat fluxes, geobotanical anomalies and Earth surface deformation. A section of this paper is dedicated to published remote sensing studies illustrating the principles of mapping: surface deformation, gaseous emissions, mineral mapping, heat flux measurements, temperature mapping and geobotany. In a case study from the La Pacana caldera (Chili) geothermal field we illustrate the cross cutting relationships between various surface manifestations of geothermal reservoirs and how remotely sensed indicators can contribute to exploration. We conclude that although remote sensing of geothermal systems has not reached full maturity, there is great potential for integrating these surface measurements in a exploration framework. A number of recommendations for future research result from our analysis of geothermal systems and the present contributions of remote sensing to studying these systems. These are grouped along a number of question lines: 'how reproducible are remote sensing products', 'can long term monitoring of geothermal systems be achieved' and 'do surface manifestations link to subsurface features'?

Introduction

Radioactively generated heat in the core of the Earth is the driver of the Earth's internal heat engine. Heat moves to the surface through conductive and convective processes. In addition, the top layer of the Earth surface is heated by solar radiation. Typical temperature gradients in the Earth crust are in the order of 25–30 °C per kilometer depth (equivalent to a conductive heat flux of 0.1 MW/km^2). However near tectonic plate boundaries specifically near diverging plate boundaries (like in active rift systems such as the mid-Atlantic rift and the East African rift), converging plate boundaries (subduction zones; Indonesia, Philippines, Chili), and along recent volcanic in intraplate settings (Hawaii, Yellowstone/US) volcanic activity results in gradients as high as 150 °C per kilometer depth. These high gradients through magma conduits trigger fluid circulation from fresh water from precipitation, ground water, lake water intrusion (meteoric water) which results in hot springs, steam vents. The amount of heat flow (heat flowing by conduction through a unit area in mW/m^2) is dependent on the temperature gradient and the thermal conductivity (in W/m °C) of the medium (rock, water).

In terms of geologic setting, geothermal systems can be classified in volcanic systems and in sedimentary systems (occurring in sedimentary basins) while another classification is in hydrothermal (water or vapor/steam dominated), hot dry rock (HDR), geopressured and magmatic (Barbier, 2002). Geopressurized reservoirs are deep (4–5 km) reservoirs in sedimentary basins that contain hot water under pressure, magmatic refers to energy stored in magma

* Corresponding author. Tel.: +31 534874353.
E-mail address: f.d.vandermeer@utwente.nl (F. van der Meer).

http://dx.doi.org/10.1016/j.jag.2014.05.007
0303-2434/

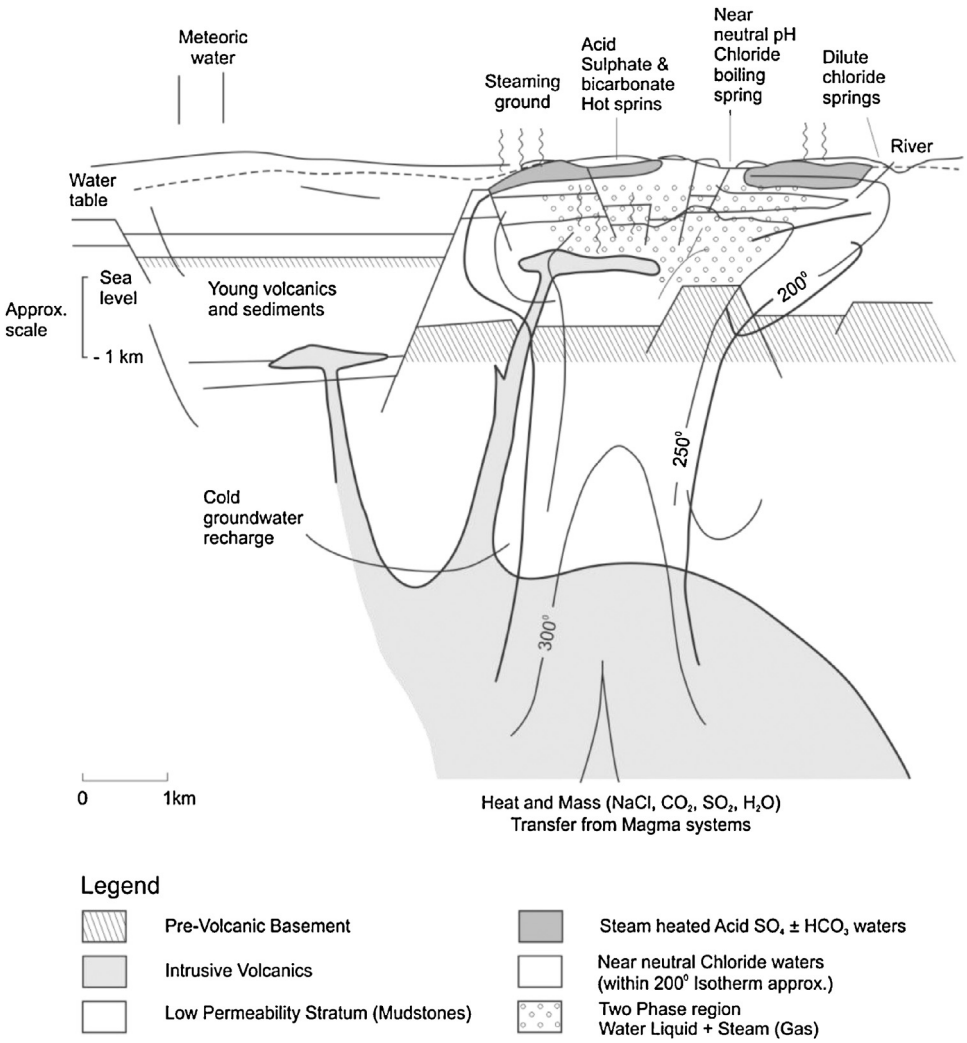

Fig. 1. Conceptual geologic model of a volcanic geothermal system where recharge results from meteoric groundwater driven by heat from supplied from a buried magmatic system leading to a convective column. Steam separation results in fumaroles and steam adsorption by groundwater while hot springs occur associated with the formation of silica.

Modified after Henley and Ellis (1983).

bodies, hot dry rock (HDR) are dry and impermeable hot rocks where by means of hydraulic fracturing ('fracking') a man-made reservoir is created.

Fig. 1 shows a conceptual model of a volcanic geothermal system. Water recharge results from meteoric groundwater infiltrating into the system driven by heat supply from a deep source of buried magmatic bodies. The magmatic body is the heat source leading to convection. Steam separation results in fumaroles and steam adsorption by groundwater which at the surface results in hot springs, steaming ground associated with the formation of silica and various alteration mineral assemblages. Gases venting from fumaroles are primarily water vapor and carbon dioxide, however also sulfurous gases are emitted.

Heat from geothermal reservoirs can be used to generate energy (electrical power) by using the steam to drive turbines in case of high temperature (>200 °C) reservoirs. Sometimes water is injected into the geothermal system to enhance the process. In case of normal geothermal gradients (30 °C/km) and low (<150 °C) temperature reservoirs, heat can be used for direct use (Lund et al., 2005) involving heating of buildings, drying of agricultural products etc. Geothermal generated energy has a number of benefits: it is renewable, it provides a stable base-load power for several decades and it is environmentally friendly with low carbon dioxide emissions compared to alternatives like fossil fuels (Mock et al., 1997). The downside maybe the emission of volcanic gases notably SO_2, CO_2 and H_2S which may be enhanced due to geothermal exploration and which are associated with respiratory mortality (Hansell and Oppenheimer, 2004). In low enthalpy systems there is the competition between aquifers used for shallow geothermal energy and for the production of drinking water. Geothermal activity gives rise to temperature variations beyond natural conditions which adversely affects groundwater quality (Bonte et al., 2013). Groundwater potentially can be polluted from reservoir fluids but also corrosion in the pipeline system used for exploration can adversely affect groundwater quality. Lastly, geothermal energy production can result in surface deformation. Lastly, geothermal energy production can result in surface deformation (Carnec and Fabriol, 1999).

Geothermal energy provides approximately 0.4% of the world global power generation with a growth rate of 5%. A good review of energy from geothermal resources is found in (Fridleifsson, 2001). At present the largest providers are in USA, Philippines, Indonesia, Mexico and Italy. To put this in perspective, solar energy plays a very limited role in global power generation (<0.2%), but it has a very high growth rate of 25–30%, especially in USA, Spain, China, Australia and India.

A recent survey (Bertani, 2005, 2012) shows that a total of 24 countries now generate electricity from geothermal resources with a total installed capacity worldwide of 10,898 MW (corresponding to about 67,246 GWh of electricity). Germany, Papua – New Guinea, Australia, Turkey, Iceland, Portugal, New Zealand, Guatemala, Kenya, and Indonesia have increased the capacity of their power plant installations by more than 50% with respect to the year 2005. The top five countries for electricity from geothermal resources are USA, Philippines, Indonesia, Mexico and Italy and the top five countries that realized an increase above 100 MW with respect to 2005 are USA, Indonesia, Iceland, New Zealand and Kenya. In addition, nearly 40 countries worldwide possess sufficient geothermal potential that could be exploited to satisfy the energy demand of the country; the largest are Indonesia, Philippines, Peru, Ecuador, Iceland, Mozambique, Costa Rica and Guatemala. In terms of installed capacity as a factor of inhabitants Iceland (>1900 MWe/mill.people) and New Zealand (150 MWe/mill.people) are world leader (USA reaches 10 MWe/mill.people). A number of scientific publications review the geothermal energy in different countries or regions including Australia (Bahadori et al., 2013), Italy (Carlino et al., 2012), Indonesia (Alzwar, 1986; Hochstein and Moore, 2008), Kenya (Tole, 1996), Turkey (Acar, 2003; Hepbasli and Ozgener, 2004), Papua New Guinea (Berhane and Mosusu, 1997), USA (Tester et al., 2007).

A geothermal project has a number of development phases: preliminary survey/site selection, exploration, test drilling, geothermal field development, power plant design, commissioning and operation. Alongside baseline environmental studies and environmental impact analysis studies are conducted. Various geological, geochemical and geophysical surveys are conducted in the exploration stage of a geothermal prospect to aid in developing a 3D subsurface model of the reservoir based on conductivity/resistivity imaging, magneto telluric methods stage and drill hole geophysics. There is ample scope for deploying remote sensing based products particular in the site selection, exploration and operational stages of geothermal reservoirs, however the use of this in not widespread.

Recently a chapter was devoted to a review of thermal infrared remote sensing systems to aid in studying geothermal systems (Haselwimmer and Prakash, 2013) and a paper was published reviewing remote sensing applications in volcanology (Ramsey and Harris, 2013). This present paper aims at investigating the role that remote sensing plays in geothermal exploration and exploitation (excluding environmental studies which are rather site specific) from which we derive trends and identify gaps resulting at recommendations for future research.

Traditional exploration methods

Traditional exploration methods are directed to finding the best suitable target locations for steam or fluid production. An initial reconnaissance survey often using airborne or spaceborne remote sensing in combination with literature study at regional scale results in a selection of a prospective area. This pre-feasibility study explores both the likelihood of the presence of a commercial geothermal reservoir, but also investigates the regional power demand, the regulatory framework, infrastructure, access to the power grid as well as environmental conditions and legislation. Remote sensing plays a role in some of these aspects, environmental base line mapping, mapping infrastructure etc., but for this paper we focus on the geologic exploration and reconnaissance stage detection of prospective areas. A good review of geothermal energy from exploration to exploitation is given in (Barbier, 2002) while classic review papers on geothermal exploration arise from geochemistry (Fournier and White, 1973; Henley and Ellis, 1983).

A hydrogeological survey aims to reconstruct the water circulation system trying to relate surface manifestations of geothermal activity (e.g., hot springs, steam vents, fumaroles, etc.) to fault/fracture systems, variation in lithology etc.

Geochemical surveys typically sample water (Arnorsson et al., 2006) from hot springs, gas from hot pools and steam from fumaroles where the fluid chemistry can be used to develop geothermometers that provide an estimate of the temperature of deep reservoirs. Suitable geothermometers exist for chlorite (Decaritat et al., 1993), illite (Battaglia, 2004), smectite-illite (Huang et al., 1993), Na/K, Na/Li and SiO_2 (Verma and Santoyo, 1997). In addition, 14C carbon isotopes provide an age on the water and thus a handle on the fluid flow, while hydrogen and oxygen isotopes are proxies for locating recharge areas.

A multitude of geophysical techniques are deployed in exploration surveys for geothermal characterization. Gravity and magnetic surveys (cf. (Bektas et al., 2007)) provide information about subsurface lithology and active seismic surveys as well as (passive) seismic tomography (Lees, 2007) provide information about subsurface structure and identification of warmer and cooler regions. Electrical methods measure resistivity (Zohdy et al., 1973) of the shallow subsurface which is related to the conductivity of the rocks which in turn is dependent on the composition, the porosity, the fill of pore spaces, and the temperature and salinity of the fluids. Electromagnetic methods in particular magnetotelluric (MT) sounding (Shoham, 1978) and the more recently introduced time-lapse MT (Peacock et al., 2013) uses natural variations of the Earth's electrical and magnetic fields to determine the depth, geometry and geologic characteristics of electrically conductive features including (clay) reservoir caps, fluid-filled reservoirs, melt accumulation in the Earth's core, fluid pathways and geothermal reservoir temperatures at depths ranging from 300 m down to several kilometers.

Reservoir modeling (see for a review (O'Sullivan et al., 2001)) integrates elements from geological, geochemical and geophysical surveying to refine the geologic model through numerical simulation. The aim is to better understand the behavior of a geothermal reservoir, to find the most suitable and productive reservoir, to estimate reservoir volume and recoverable heat, to identify zones of high permeability, to locate drilling locations, and to forecast future well and reservoir behavior.

Measurable variables by remote sensing

Introduction

Hydrothermal alteration of rocks relates to changes in mineralogy, texture and rock chemistry as a result of changes in temperature (and pressure) and chemistry of the environment resulting from interaction with hot water, steam of gas in a geothermal system. Consequently the temperature, Ph and chemical composition of the brines, in volcanic systems often recharged meteoric water, determine the mineral alteration. For the ease of summarizing, we consider direct evidence of geothermal activity at the surface and indirect evidence of geothermal activities. We consider evidence 'direct' if it can be directly related to geothermal activity based on the underlying physical processes while 'indirect' evidence would require further interpretation to make the link to geothermal activity evidential.

Direct evidence

Direct evidence for geothermal activity as can be retrieved from remote sensing are through surface features and anomalous mineral assemblages. Surface features of geothermal activity that can be retrieved and mapped from remote sensing include caldera

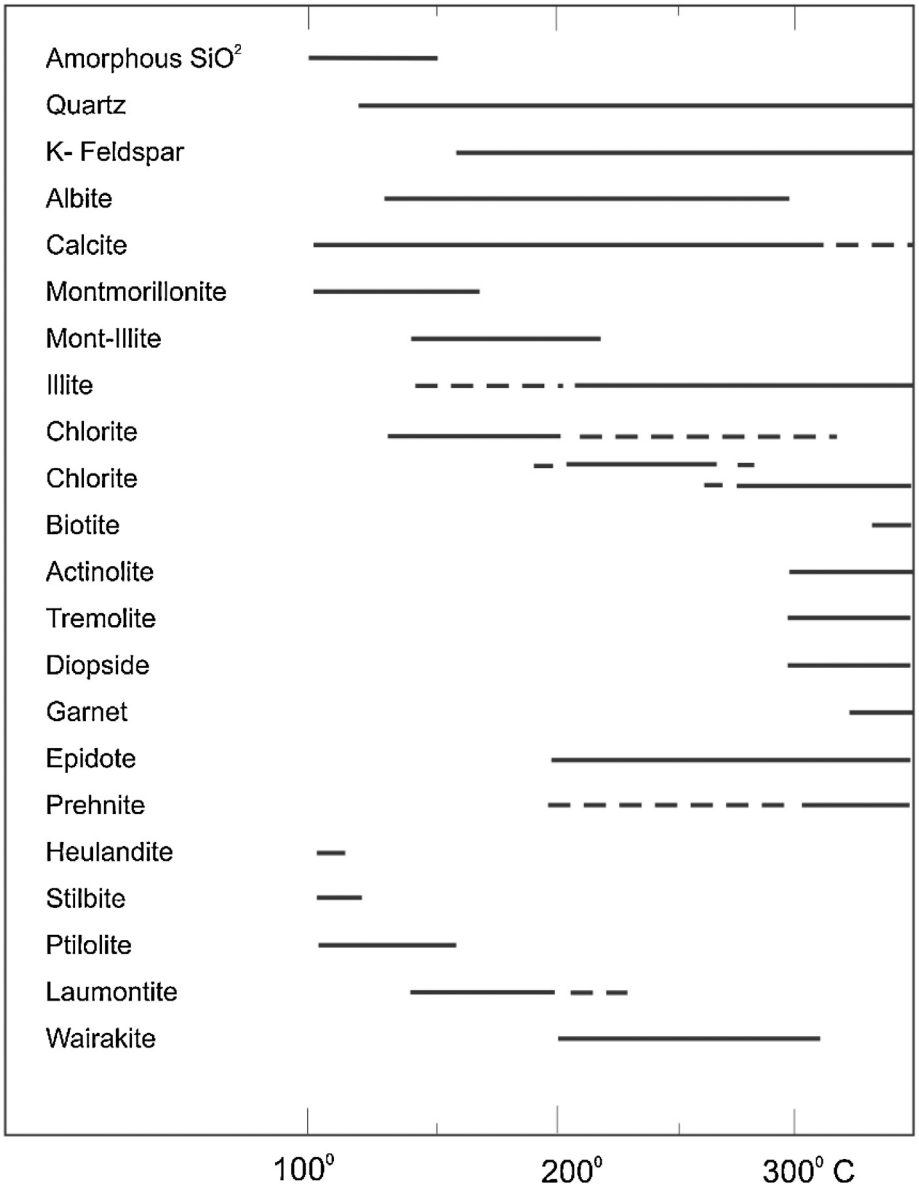

Fig. 2. Overview of key alteration minerals associated with geothermal systems and their temperature stability. After Henley and Ellis (1983).

structures, hot springs, steaming ground, and fumaroles. Often there is a structural control on the location of geothermal surface manifestations thus fault and lineament mapping are also pre-requisites. Geothermal areas often have a distinct signature in terms of surface mineralogy. In addition to the chemistry of the brines interacting with the host rock through which fluids are circulating, the reactivity of minerals present in these host rocks to alteration varies considerably. Quartz is almost inert, while volcanic glass is most reactive. A summary of stability of aluminum-silicate alteration minerals in relation to the temperature of the brines is provided in Fig. 2. In the case study, see Section "A case study: the La Pacana caldera (Chili) geothermal field", we provide an example of silica mapped from ASTER (the Advanced Spaceborne Thermal Emission and Reflection Radiometer) data.

In the lower (around 100 °C) temperature ranges zeolites and montmorillonite is stable, at 200 °C illite appears and at temperature in the range of 300 °C waikarite (a hydrated calcium aluminosilicate zeolite mineral typically found near hot springs) appears. In calcite-rich systems, above 250 °C epidote appears while above 300 °C calcite is altered to actinolite and diopside. In the case study of section "A case study: the La Pacana caldera (Chili) geothermal field" we provide examples of mapping clay mineral alteration related to geothermal activity (Fig. 4). An additional control on the stability of calcium-rich minerals is the concentration of CO_2 in the geothermal fluids. The near-surface part of the steam-heated zone is often characterized by the presence of alunite, kaolinite and iron oxides, while in more sulphur-rich environments also pyrite occurs. Remote sensing can make a valuable contribution to mapping the spatial extent of surface geology and mineralogy. Multispectral broad band remote sensing can be used to map broad classes of surface mineral facies while with hyperspectral optical remote sensing surface mineralogy maps can produced (van der Meer et al., 2012).

Indirect evidence

Variations in surface temperature in relation to the presence of heat sources as well as heat fluxes can be readily measured

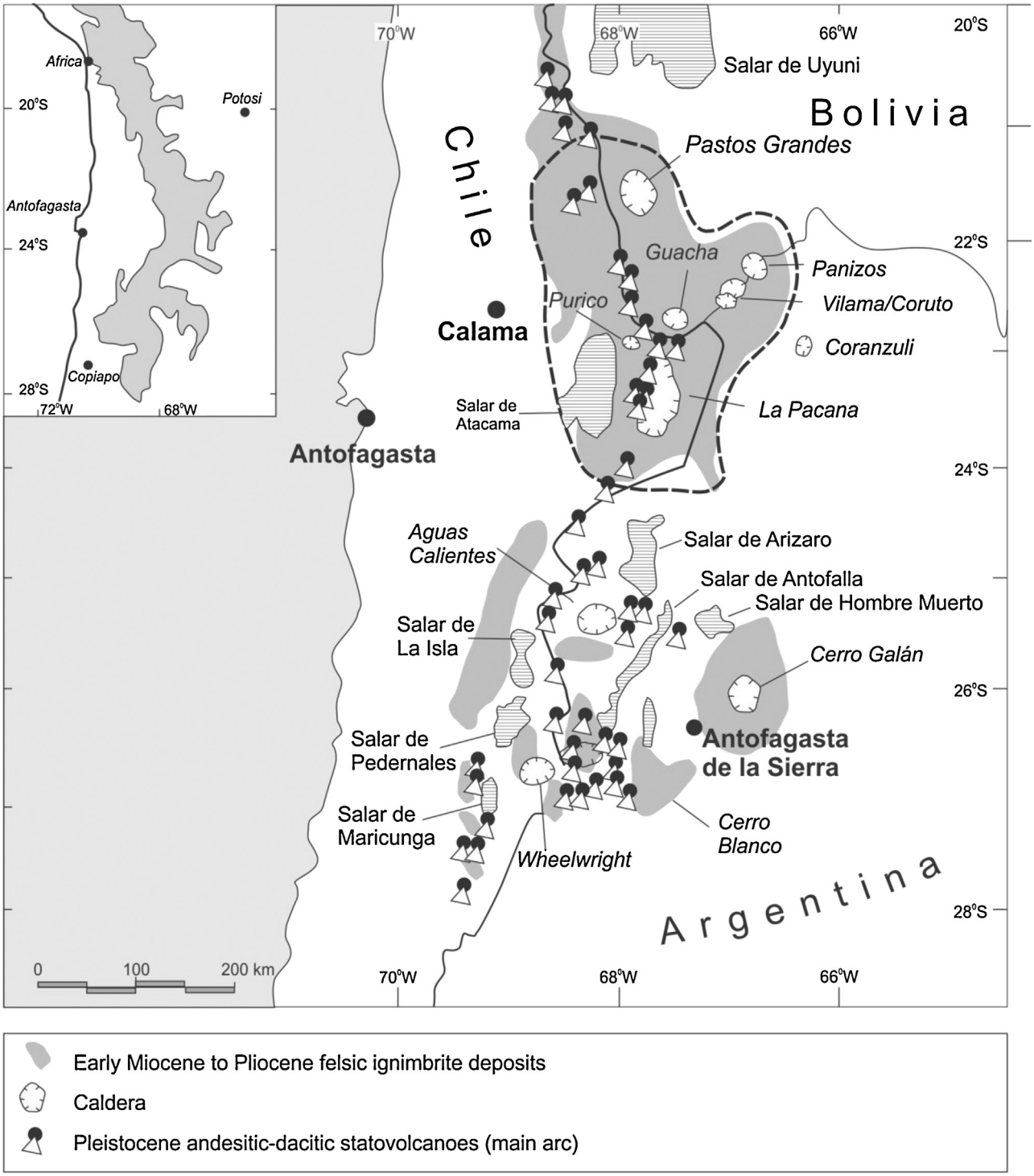

Fig. 3. Geologic map of the Central Andes of Chili showing the location of the geothermal system studied. After Schnurr et al. (2007).

and mapped using thermal infrared radiation. In addition, surface deformation related to geothermal activity can be retrieved using SAR interferometry. This is relevant during exploration particular in enhanced (by hydraulic fracturing) geothermal systems but literature (Majer et al., 2007) suggests that microseismicity (and surface deformation) also is a natural phenomena in geothermal systems possibly related to seasonality or other external driven factors. For example, a number of effects on the vegetation can be anticipated in relation to geothermal activity. Accumulation of geothermal gases such as SO_2, H_2S and CO_2 in the soil has adverse effects on the phenological functioning of plants. A clear negative correlation between soil CO_2 and plant height and leaf chlorophyll has been found by several authors (Noomen and Skidmore, 2009; Vodnik et al., 2006). Toxic gas release and soil acidification also

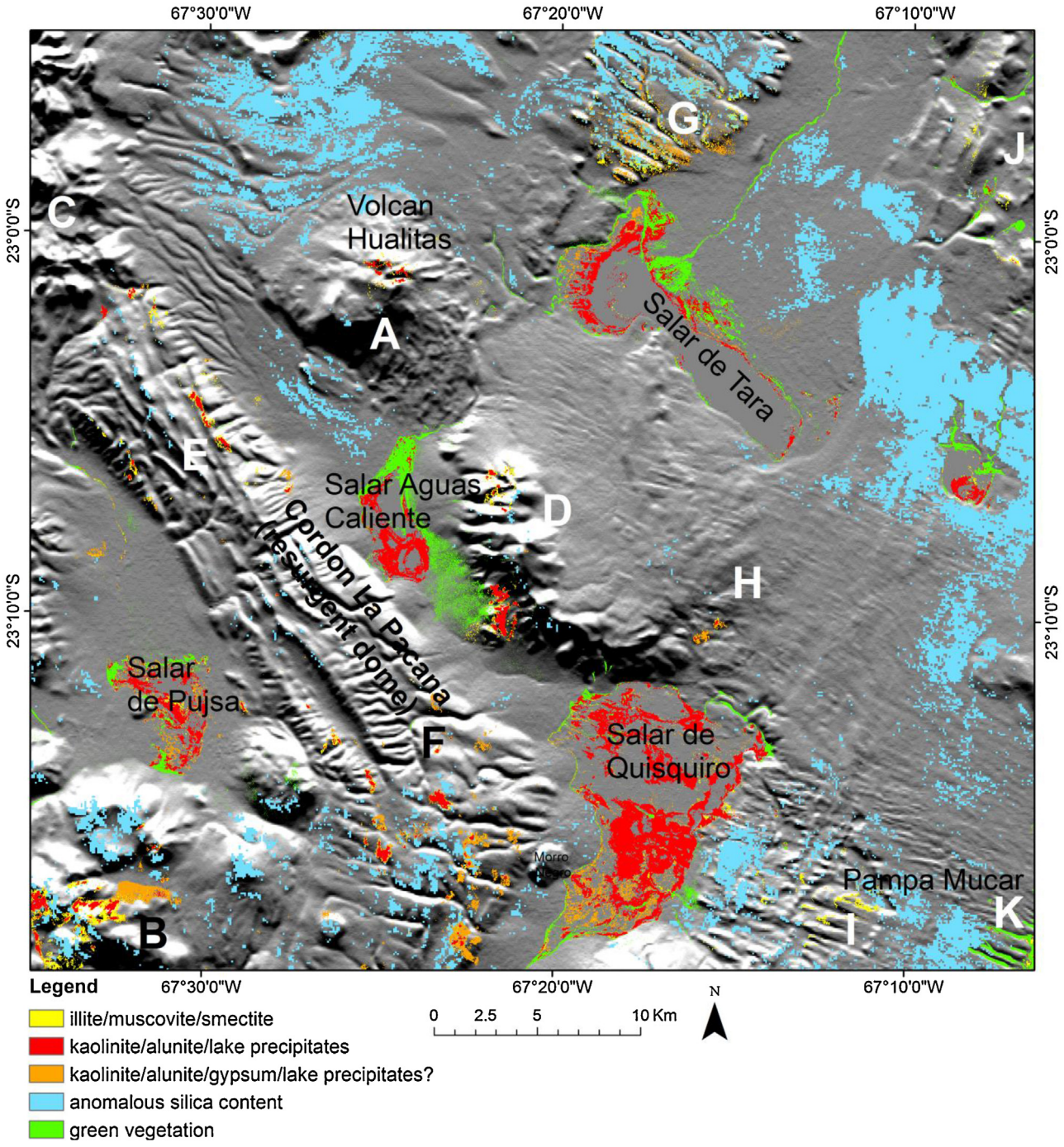

Fig. 4. Classification of the ASTER daytime imagery showing various groups of minerals and vegetation. Hill shaded SRTM image used as background (symbols A–K are explained in the text). (For interpretation of the references to color in this figure legend, the reader is referred to the web version of the article.)

has been shown to result in vegetation stress (Nash et al., 2003) and decrease in species richness, leaf size, and rooting depth in geothermal fields.

Remote sensing of geothermal fields; examples and case studies

Background

In this section we provide a review of existing applications of remote sensing data in studying geothermal fields. The geologic remote sensing community has contributed many papers to the study of fossil hydrothermal systems. An early review of the used of remote sensing in studying hydrothermal systems is (Huntington, 1996). The launch of ASTER, the Advanced Spaceborne Thermal Emission and Reflectance Radiometer, provided enhanced mineral mapping capabilities for the geologic remote sensing community which resulted in several studies of hydrothermal systems (Carranza et al., 2008a; Crosta et al., 2003; Hubbard et al., 2003; Mars and Rowan, 2006, 2010; Rowan et al., 2003). The improvement of signal to noise and increased spectral resolution of hyperspectral remote sensing instruments, which due to their high spectral resolving power allow to map detailed spectral absorption features intimately linked to mineralogy, has resulted in many studies

on mineral mapping in fossil hydrothermal systems (Bedini et al., 2009; Kruse, 2012; van der Meer et al., 2012; van Ruitenbeek et al., 2005).

Some of the early studies on remote sensing in relation to geothermal resources date back to the 1980s en 1990s. The first projects focused on helicopter-based mapping of geothermal area (Sekioka, 1985). Several early studies focused on the geothermal areas in New Zealand. The first study using nighttime airborne thermal infrared data focused on temperature mapping of hot springs (Mongillo, 1994), while Landsat and SPOT (Satellite Pour l'Observation de la Terre) data were used to map structures related to geothermal processes (Deroin et al., 1995). The various contributions of remote sensing to geothermal research can be grouped under the headings: surface deformation, gaseous emissions, structural analysis, mineral mapping, surface temperature mapping, heat flux mapping and geobotany.

Surface deformation

There are several studies of geothermal sites with interferometric (Synthetic Aperture Radar) SAR aimed at monitoring land subsidence and surface deformation. Most of these measurements are done with ERS (the European Remote Sensing Satellite) and ASAR (Advanced Synthetic Aperture Radar) data and with the launch of the ESA (European Space Agency) sentinel-1 mission (Snoeij et al., 2010) it can be perceived that such measurements will be done routinely in future geothermal projects. Examples include the subsidence of the Cerro Prieto field (Mexico) as a result of withdrawal of geothermal fluids (Carnec and Fabriol, 1999), deformation of the surface linked through inverse modeling to monitor pressure changes in geothermal reservoirs at depth (Fialko and Simons, 2000) and a study on surface features of depressions in the Vatnajokull ice cap (Iceland) resulting from geothermal heating (Jonsson et al., 1998). Recently a number of articles (Lubitz et al., 2013; Sass and Burbaum, 2010) were published on a geothermal exploration site near the city of Staufen (Germany) where a number of uncased boreholes (140 m deep) were drilled into anhydrites creating a contact with the groundwater. Anhydrite transforms into gypsum when in water and as a result the volume increases up to 61%. This in turn resulted in pressures that led to uplift and subsequently damage to buildings in the town.

Gaseous emissions

A number of projects attempted to quantify gaseous emissions from geothermally active areas. The Latera caldera a dormant volcanic structure in Central Italy was analyzed with a combined multispectral (Airborne TM and CASI, the Compact Airborne Spectrographic Imager Canadian hyperspectral instrument), hyperspectral (Specim Eagle) and LIDAR (Light Detection and Ranging) data with an attempt to map CO_2 from vents (Bateson et al., 2008) yielding a maximum of 47% success rate. In another project, a terrestrial thermal infrared camera provided image data that allowed to detect CO_2 vents and also to determine gas quantities emitted (Tank et al., 2008). The method for the first time allowed CO_2 flux quantification from infrared image time series, however no attempt has been made to repeat this from airborne measurements for vents related to geothermal activity. There is a wealth of literature in Abrams et al. (2013), Pieri and Abrams (2004).

Structural analysis

Reconstructing the relation between the stratigraphy and structural geology of a geothermal area in relation to the hydrogeology is important for unraveling the functioning of cap rock, reservoir and circulation of geothermal fluids. Combined use of multispectral enhanced image products and products derived from digital terrain models derived from either SAR or LIDAR data sets have been demonstrated for structural mapping by various researchers. Examples of such studies are from the Cerro Tuzgle–Tocomar geothermal volcanic area in Argentina (Giordano et al., 2013), the Kenyan rift (Kuria et al., 2010), hot springs in Taiwan (Liu et al., 2003).

Mineral mapping

There is a wealth of papers on surface alteration mineralogy mapping using both multispectral and hyperspectral data sets. Particularly the advent of ASTER has resulted in an exponential increase in papers on this topic. In the case study in section "A case study: the La Pacana caldera (Chili) geothermal field", our Fig. 4 provides a ASTER based mineral map as an example product. Some of the more fundamental work on spectroscopy of alteration mineralogy related to geothermal activity addressed the issue of loss of nitrogen in a oxidizing supergene environment resulting in a carbonate-low anomaly above buried geothermal systems as witnessed by late stage formation of the ammonium feldspar buddingtonite (Krohn et al., 1993). More recently a number of examples of shortwave- and long wave infrared hyperspectral analysis of geothermal systems to map alteration mineralogy was presented (Kruse, 2012). A classic paper using the MODIS/ASTER airborne simulator, MASTER (Hook et al., 2001), and SEBASS (Hackwell et al., 1996) data (Spatially Enhanced Broadband Array Spectrograph System; a hyperspectral thermal instrument) to combine (shortwave infrared) SWIR and (long wave infrared) LWIR to map alteration in the Steamboat Springs geothermal system unraveled the geothermal history of the area by showing the spatial distribution of (quartz-rich) sinter related to recent geyser activity, hydrous Na–Al sulfates forming crusts around active fumaroles, and steam heated sulfate alteration related to past geothermal activity (Vaughan et al., 2005). Combined use of ASTER and HyMAP (the Hyperspectral Mapper airborne hyperspectral) data allowed to map alunite, kaolinite, montmorillonite/illite, chlorite, and carbonate at the Pyramid Lake geothermal site. By integrating these image products in a structural geologic context the authors were able to relate alteration mineralogy to geothermal activity (Kratt et al., 2010). In general, ASTER allows to make a first regional reconnaissance inventory of surface mineral alteration features leading to the identification of prospective areas for geothermal exploration. With hyperspectral data such as HyMAP or AVIRIS (the Airborne Visible/Infrared Imaging Spectrometer) one can add the minerologic detail. The Yellowstone National Park geothermal area has been extensively studied using remote sensing. The fact that there are over 10,000 geothermal surface manifestations spread out over 5000 km^2 (Vaughan et al., 2012) makes remote sensing the obvious choice. Using a combination of airborne, AVIRIS, and spaceborne, ASTER, data the active and extinct hot springs could be mapped (Hellman and Ramsey, 2004). In a recent paper, combined use of AVIRIS, HyMap, and ProSpecTIR data were used to derive mineral maps over the Fish Lake Valley (Nevada, US) resulting in new insights into the geothermal prospectivity of the area (Littlefield and Calvin, 2014). In a recent paper, hyperspectral thermal data from SEBASS was used to map alteration mineralogy associated with geothermal activity in the Salton Sea geothermal area (Reath and Ramsey, 2013). A good overview of hyperspectral remote sensing and geothermal prospecting reviewing the state-of-the-art up to around 2000 is found in Martini et al. (2004), Martini et al. (2003). Another noteworthy study focused on mapping soil mineral anomalies in the Dixie Valley geothermal area using hyperspectral data (Nash et al., 2004).

There have also been publications on data-driven evidential belief functions in GIS-based predictive mapping to exploit the spatial association of geologic features (lithology, mineralogy,

structures) and occurrences of geothermal manifestations. In general, these predictive mapping approaches use a number of known occurrences of geothermal activity and make a spatial correlation to these features using a number of geologic layers such as faults, lithology etc. This expresses the control that these geologic features have on the occurrence of a geothermal feature. The next step is the forward modeling where the predictive models calculates the probability of a geothermal feature to occur based on the combination of a number of geologic parameters in an area. A case on a geothermal field in West Java, Indonesia, properly predicted 94% of the geothermal occurrence (Carranza et al., 2008b) however using exploration data sets as evidence layers. Another weights-of-evidence model (Coolbaugh et al., 2005) included gravity gradient, crustal strain, earthquakes, and isostatic gravity as evidence layers as these are independent of the exploration data sets and thus unbiased estimators. This allowed these authors to assess the undiscovered geothermal resources and assess the thoroughness of past exploration efforts geospatially.

Temperature

There are a number of papers demonstrating the use of TIR (thermal infrared) data to map surface temperature and correlate that to geothermal heat. A fundamental paper proposing a comprehensive processing chain using ASTER day- and nighttime images investigated surface materials with different physical properties showing the physical relationship between thermal inertia, albedo, emissivity, and moisture content to surface temperature during a diurnal cycle (Coolbaugh et al., 2007). These authors, acknowledging that surface radiant temperature is negatively correlated to emissivity, developed (in part) empirical relationships to correct for surface albedo and topographic slope showing that the derived surface temperature product was more easily interpretable in relation to geothermal sources (Coolbaugh et al., 2007). Another fundamental paper simulated ASTER TIR data derived thermal anomalies to see what size versus temperature anomaly can be measurement assuming that geothermal heat sources typically are of subpixel size (Vaughan et al., 2010). Some authors also pointed out that the effect of elevation should be treated with due care in the interpretation of temperature data to ensure false anomalies are filtered out (Eneva and Coolbaugh, 2009). Other examples of the use of surface temperature derived from TIR remote sensing data include geothermal complexes in the Andes of Central Chile using ASTER data (Gutierrez et al., 2012), a study on the Tengchong area (Yunnan province) in China using Landsat-7 Enhanced Thematic Mapper+ (Qin et al., 2011) and a study on temperature linked to fault controlled hot springs in Gulf of Suez (Egypt) waters (Kaiser and Ahmed, 2013). In the Chilean case study we provide a ASTER based temperature map (Fig. 5) and a temperature map corrected for average background variations (Fig. 6) as a proof of concept.

Heat flux measurement

Besides surface temperature there are also several studies investigating the potential of TIR remote sensing data to estimate the geothermal heat flux (GHF). A processing chain for Landsat ETM+ based GHF was presented in 2008 (Watson et al., 2008) and later refined (Savage et al., 2010). Using combined ASTER and MODIS (e.g., the Moderate Resolution Imaging Spectroradiometer) acquisitions a processing chain was developed for radiant geothermal heat flux that allowed to identify background changes and seasonal effects to allow a better extraction of geothermal anomalies (Vaughan et al., 2012). In general ASTER TIR data (90-m pixels) is used to estimate the radiant GHF while the MODIS TIR data (1-km pixels) allows to produce time series to record background thermal radiance variations. Another noteworthy paper on GHF uses estimates from high-spatial resolution airborne TIR data to measure outflow rate of hot springs in the Western Canadian Pilgrim geothermal system (Haselwimmer et al., 2013).

Geobotany

There is surprisingly little published research on the relation between vegetation species distributions, vegetation health status, phenology and geobotany and geothermal surface manifestations although it is generally accepted that anomalous soil chemical conditions resulting near geothermal vents must influence the vegetation. Spatial variation of soil temperature gradients has been shown to influence vegetation communities. In the Te Kopia geothermal field in the Taupo Volcanic Zone (New Zealand), for example, the dominant species changed from broadleaved evergreen forest to shrubs when approaching a steam field (Boothroyd, 2009; Burns, 1997). Likewise it has been shown that density of lichen coverage of rocks correlates negatively to surface temperature (Fahselt, 1995). Optical multi- and hyperspectral remote sensing offers potentially a tool to map vegetation parameters that can be related to vegetation species diversity and vegetation stress. Using field spectral measurements along transects over known geothermal manifestations a comprehensive set of independent estimates of plant stress (e.g., the 'red edge' position, the R699/R765 ratio values) a clear relation between healthiness of vegetation and geothermal occurrences was shown (Nash et al., 2003).

A case study: the La Pacana caldera (Chili) geothermal field

To illustrate a number of aspects related to the use of earth observation in the reconnaissance stage of geothermal exploration we provide a case study from a prospect in the Chilean Andes. This case study shows how ASTER can be used to aid in mineralogic mapping and how result can be integrated with surface temperature maps to derive anomalous areas that require potential follow up for exploration.

The geothermal system of study is the La Pacana caldera located in the Neogene magmatic arc in the Central Andes range of Chili (Fig. 3). There have been several publications on the Pacana caldera (Kay et al., 2010; Lindsay et al., 2001a,b; Schnurr et al., 2007) however no extensive studies on geothermal aspects and few studies on remote sensing in the area (Bailey et al., 2007). We use ASTER daytime and nighttime images to conduct a comprehensive geologic interpretation of the mineralogy and emissivity features related to geothermal activity in the area.

Pre-processing

Two ASTER (processing L1B) images were used: one daytime image acquired on 22 December 2006 and one nighttime image acquired on 24 November 2011. For the mapping of thermal anomalies, nighttime ASTER images were used. In daytime images, differential solar heating (due to e.g., slope angle and aspect, albedo of the materials) can greatly influence the distribution of thermal patterns and often swamps out subtle temperature differences due to geothermal activities. Nighttime imagery is less influenced by this effect and the contrast between anomalies and background ground temperature is enhanced. Several nighttime ASTER scenes were investigated but seasonal variations appeared to be minimal.

The ASTER satellite imagery was corrected for crosstalk effects using the tools provided by ERSDAC (http://gds.aster.ersdac.jspacesystems.or.jp/gds_www2002/service_e/u.tools_e/set_u.tool_e.html). Subsequently all 14 bands were converted to radiance at sensor by applying gain factors. Bad edges were removed from the imagery. The bands were stacked and resampled to 15 m

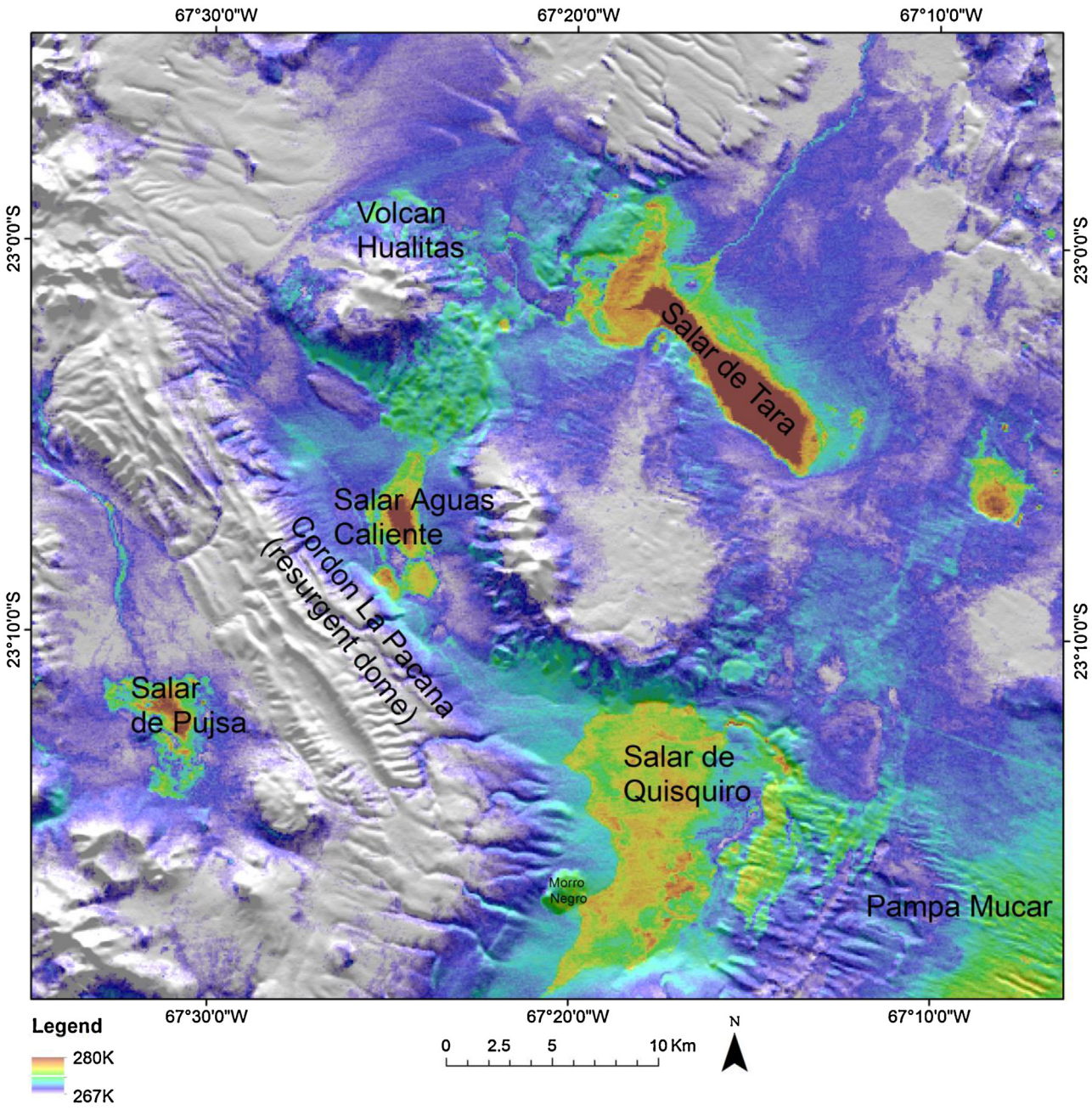

Fig. 5. Surface temperature map derived from ASTER nighttime imagery. Hill shaded SRTM DEM in background. (For interpretation of the references to color in this figure legend, the reader is referred to the web version of the article.)

resolution. The radiometric and geometric corrected images were atmospheric corrected and converted to pseudo-reflectance using the log residuals method. This method corrects for albedo differences, shape of solar curve and systematic atmospheric effects. The method involves normalization to average radiance of pixel and a second normalization to the mean pixel-spectrum of the scene, both in logarithmic space. To compensate for atmospheric effects, In-Scene Atmospheric Compensation (Young et al., 2002) was applied to the five ASTER TIR bands, where ISAC estimates atmospheric transmission and up-welling sky radiance directly from the dataset itself. After ISAC compensation the 5-band radiance data were separated into ground temperature and ground emissivity using an Emissivity Normalization algorithm (Kealy and Hook, 1993).

Mineral mapping

Daytime ASTER satellite imagery was used to map clay and other alteration minerals, silica anomalies and green vegetation. Using band ratio techniques for enhancement of absorption features and studying (pseudo) reflectance curves three different mineral assemblages were identified in the image.

Three mineral assemblages were identified and mapped:

(1) endmember 1 has a deep feature near 2.20 μm (band 6) which is indicative for absorption by Al—OH groups and is interpreted as an assemblage that likely contains illite/muscovite/smectite minerals and may represent argillic alteration (endmember 1)

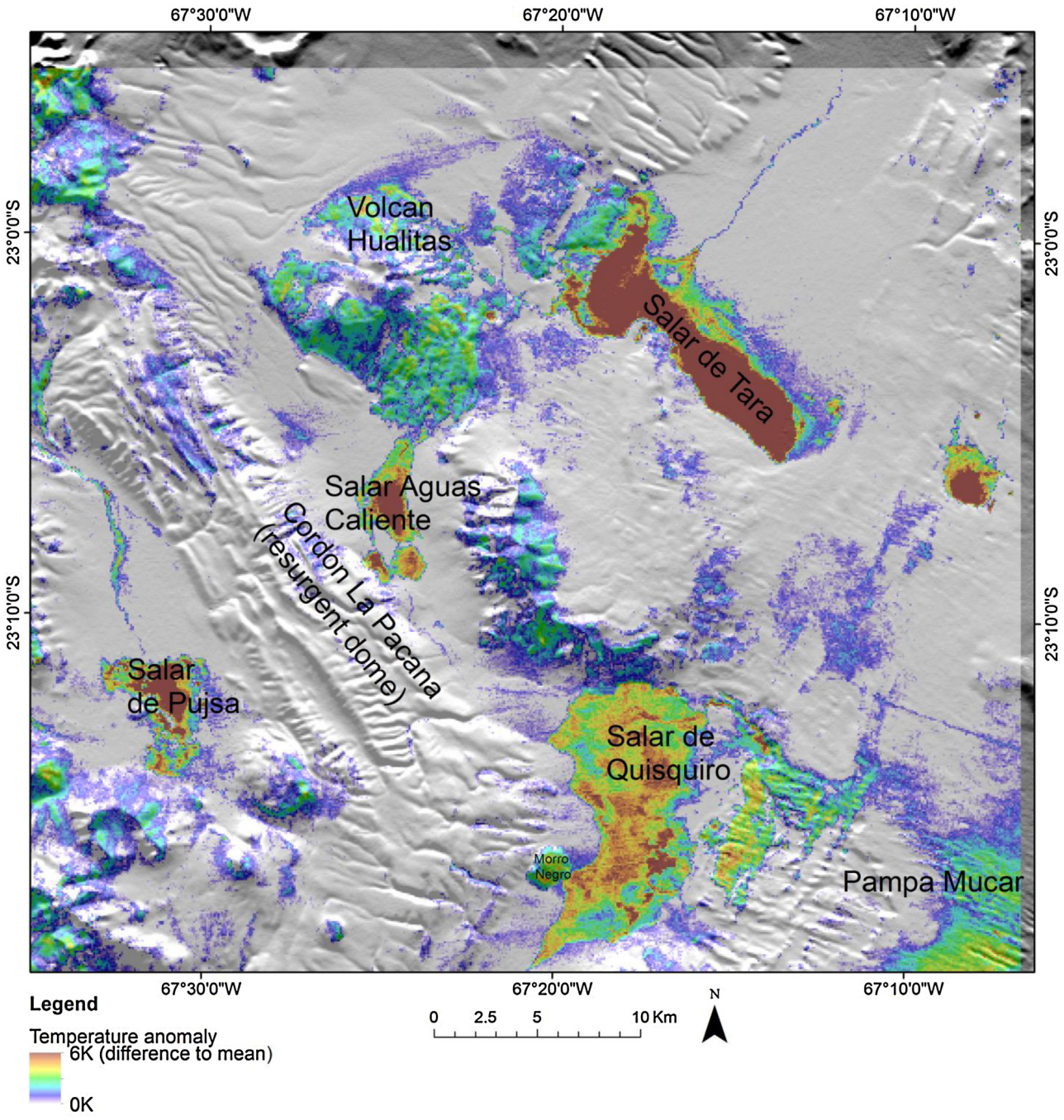

Fig. 6. Temperature anomaly map using the method of (Ulusoy et al., 2012) based on ASTER nighttime imagery. Hill shaded SRTM DEM in background.

(2) endmember 2 has deep absorption in both 2.16 and 2.20 μm (bands 4 and 6 respectively) and is often related to Al—OH bonds in phyllosilicates this is interpreted as an assemblage that likely contains kaolinite/alunite/lake precipitates and may represent advanced argillic alteration (endmember 2)
(3) endmember 3 is a spectrum that has a shallower absorption feature than that of end member 2 and the absorption near 2.16 is deeper than that near 2.20 μm which is interpreted as an assemblage that probably contains kaolinite/alunite/gypsum/lake precipitates (endmember 3).

End members were matched to the image spectra using the spectral angle mapper method and the resulting rule images were thresholded (using end member 1: <0.02 radians, end member 2: <0.05 radians, end member 3: <0.02 radians). Classification result is shown in Fig. 4, where end member 1 is shown in yellow, end member 2 in red and end member 3 in orange. The response in the lake sediments may not be reliable because of the very high albedo of some of these sediments. Clay minerals assemblages occur at several places in or near the San Albert license areas. Indication of argillic and advanced argillic alteration were found within andesitic edifices of Volcan Hualita, Cerro de Pili, Cerro Incaguasi Norte, and the andesite center east of Salar Aguas Caliente (Fig. 4A–D). The Atana ignimbrite forming the Cordon La Pacana also contains clusters of fault controlled hydrothermal alteration zones (Fig. 4E and F). Several layers within the Tara ignimbrite that are exposed near G in Fig. 4 also contain indications of clay minerals. Advanced argillic alteration is also present in the Tara ignimbrite near H in Fig. 4.

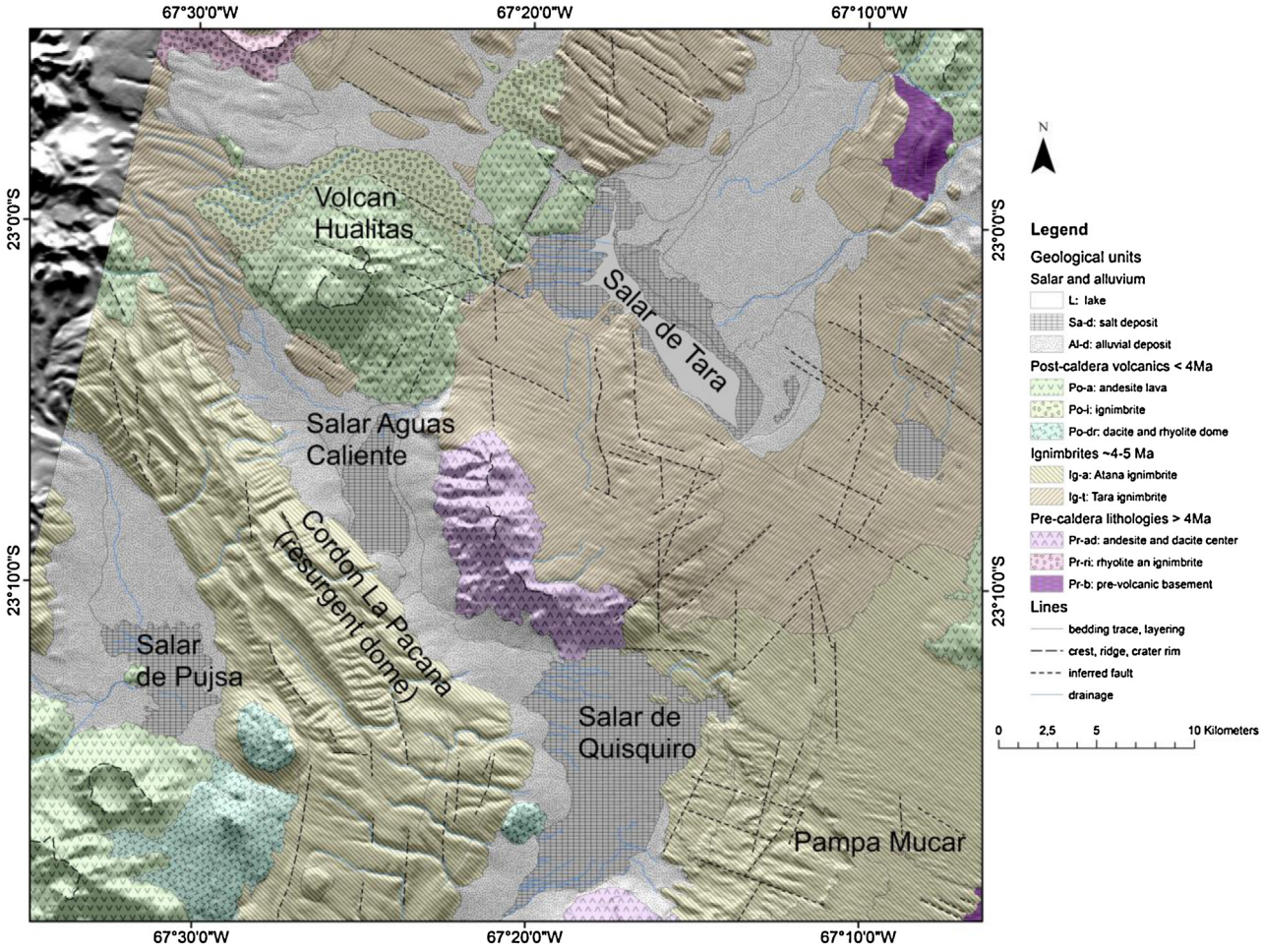

Fig. 7. Geology of La Pacana caldera and Atana ignimbrite using hill shaded STRM DEM as backdrop on ASTER daytime imagery. (modified after Gardeweg and Ramírez (1987)).

Layers in the Atana ignimbrite that are exposed by weathering of the overlying layers contain clay minerals in the southeast of the study area (Fig. 4l). Basement rocks of sedimentary origin that are exposed near J and K in Fig. 4 contain phyllosilicates, such as white micas and clay minerals.

In order to map silica-rich rocks, a band ratio in the ASTER TIR bands was used that highlights the Reststrahlen feature (a low in its emissivity spectrum) of silica minerals. From literature several band ratios have been used in the past. In this study we used two band ratios to highlight (b10/b12 and b13/b12) the silica feature. Silica anomalies show both broad and more localized patterns. The first related to a higher silica content of the volcanic rocks and the second may be related to localized hydrothermal or volcanic activity. Vegetation abundance is related to availability of water in streams, lakes and spring activity. Daytime ASTER satellite imagery was used together with SRTM elevation data to interpret lithological units and structures. Comparison with geological literature of the area resulted in a division of several groups of (mostly volcanic) units into pre-caldera lithologies older than 4 Ma, a group of ignimbrites that includes the Atana ignimbrite that was produced before and during the La Pacana caldera formation between 4 and 5 Ma and the Tara ignimbrite deposited in the same period from a different volcanic source, and post-caldera volcanic units younger than 4 Ma. Signs of hydrothermal alteration occur within the different units. Structures are predominantly striking northwest-southeast to north-south and northeast-southwest orientation also occurs. The Cordon La Pacana is more faulted and was interpreted as a resurgent dome after the collapse of the La Pacana caldera.

Temperature anomalies

The resulting temperature image from the ASTER TIR data shows the estimated ground temperatures in the study area (Fig. 5). The values are stretched from 267 K (blue) to 280 K (reddish brown) absolute temperatures (white areas have temperature values of <267 K). The values can be interpreted directly as integrated ground temperatures over a pixel size of 90 m × 90 m. The highest temperatures in the image are reached in lakes, with a maximum temperature of 285.6 K (about 12.5 C) in the SE part of the Salar de Tara. Little streams (and vegetated areas alongside them) also show higher nighttime temperatures than surrounding materials. This is caused by the higher heat capacity of surface water, vegetation and moist soil, making them cool down slower at night than solid rocks or dry soils. In most cases temperatures of hot springs cannot be estimated directly from the nighttime temperature image, since the areas covered by warmer water temperatures are often minor compared to the footprint of an ASTER pixel.

In the surface temperature image derived from the ASTER TIR bands (Fig. 5) the tops of volcanoes are showing very low temperature values due to temperature lapse rate (change of temperature with increase in altitude) and steep flanks of volcanoes show increased temperature due to residual differential heating during

the day. To correct for these effects we use an empirical topographic temperature correction (Ulusoy et al., 2012) that uses terrain elevation from SRTM elevation as well as its derivatives slope and aspect to develop empirical relationships between the topographic parameters and the measured surface temperature. This result is a relative temperature map (with temperature as anomaly relative to the mean temperature) with the effect of topography subdued and in part removed (Fig. 6). The resulting image (Fig. 6) covers a smaller area as its input ASTER temperature product because the correction algorithm deploys square images without missing values. The output map shows relative temperature differences to the scene mean. Some of the patterns have remained the same as in the uncorrected version (lakes and vegetation is warm), however, in hilly areas, the temperature patterns are more coherent and artifacts due to altitude or slope are strongly reduced.

Validation and interpretation

For reference, the interpreted geologic map modified after an existing published map (Gardeweg and Ramírez, 1987) is provided in Fig. 7. The discussion below refers to units listed on this map. Pre-caldera lithologies are considered older than the main eruption event and subsequent collapse of the La Pacana caldera. The ~4–5 Ma Atana ignimbrite resulted from the eruption of La Pacana caldera while the Tara ignimbrite resulted from volcanic eruptions north of the La Pacana crater (Lindsay et al., 2001). The two types of ignimbrites are difficult to differentiate using the remote sensing data sets. The Cordon La Pacana in the southwestern quadrant of the mapped area was interpreted as a resurgent dome after the collapse of the La Pacana caldera. Post-caldera volcanics are younger than 4 Ma and include various suites of volcanic rocks and alluvial deposits.

All interpreted faults were classified as inferred faults because of the lack of ground truthing information. The dominant direction of structures is northwest-southeast. This direction is also visible as regularly spaced lineaments throughout the outcrops of the Atana and Tara ignimbrites outside the Cordon La Pacana. The Cordon La Pacana is structurally different from the other rocks in the area since it is tilted, faulted and folded (and forms an anticlinal shape in the southern part of the study area) interpreted as a resurgent dome.

From the mineral maps it is difficult to judge whether the clay alteration is related to fossil or active hydrothermal/volcanic activity. Systematic comparison with the temperature anomaly map and further investigation in the field is needed to determine which mineral altered areas are linked to active and which ones to fossil geothermal systems.

The temperature and temperature-difference (compared to the mean) were validated using field temperature probe data (Fig. 8). There seems a reasonable correspondence between ASTER derived temperature and the field-based probe data. Some assumptions we needed to make hamper the comparison. The temperature probe data were taken at 50 cm depth and can be considered point measurements compared to the integrated surface temperatures over a 90 m × 90 m ASTER pixel area. The probe data were also collected on a different date and time of day, potentially causing deviations due to differences in thermal conductivity and heat capacity of the lithologies involved. Changing soil moisture can be an additional source of variation in heat capacity, although in this arid climate it is likely that the soil moisture content away from surface water and hot springs are evenly low. Furthermore, the ASTER image was not corrected for heat capacity and albedo differences of the lithologic units. Nevertheless, the ASTER temperature anomalies showed no link to the albedo of the materials they occurred in, and the results look promising.

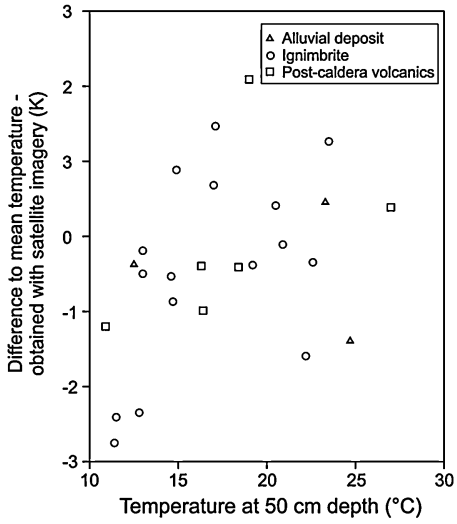

Fig. 8. Comparison of Temperature anomalies based on ASTER nighttime imagery and field-based temperature probe data.

Discussion and future prospects

Traditional exploration of geothermal reservoirs is done using subsurface imaging (using geophysical techniques) as input to reservoir modeling with limited use of field data besides the geochemical analysis of brines and hot springs. Earth observation, although this is a trivial remark addressing a remote sensing community, adds the geospatial component to the equation (earth surface information) as well as the time domain. Optical multi- and hyperspectral remote sensing can aid in better understanding surface geology and mineral alteration related to geothermal activity, thermal remote sensing allows to measure and map surface temperature distribution and heat flux, while with instruments like MODIS we gain insight into long-term thermal radiance variations. InSAR data can add information on earth surface deformation, subsidence/uplift, which can be coupled to the development of the reservoir through reservoir modeling. However a number of steps need to be taken for a full uptake of remote sensing in geothermal exploration.

A number of recommendations for future research can be drawn from our analysis of geothermal systems and the present contributions of remote sensing to studying these systems. These are grouped as follows along a number of question lines:

- how reproducible are remote sensing products?

  The geologic remote sensing community has contributed to a better understanding of geothermal systems by studying surface mineralogy using both multi as well as hyperspectral data. In case of multispectral data the products were mostly based on image ratio, for hyperspectral data a wealth of spectral mapping techniques are available to map surface mineralogy. An attempt to develop automatic procedures for hyperspectral mineral mapping is the USGS tetracorder expert system (Clark et al., 2003). However these mineral maps are of low technology readiness level (TRL) because there is a lot of human bias in setting parameters for the algorithms as well as a lot of interpretation involved to distil geology out of these products. Surface temperature retrieval and the retrieval of heat flux are based on data assimilation and physical modeling which inherently are more reproducible although subject to some boundary conditions and often empirical relationships in the models. Likewise surface deformation measurements from InSAR are based on physical principles that are 100% reproducible.

- can long term monitoring of geothermal systems be achieved?

Acknowledging that geothermal systems are dynamic and exploration potentially accelerates certain associated processes it is apparent that long-term monitoring is required. Long-term monitoring of surface deformation with SAR interferometry is secured through the advent of sentinel-1 mission (Snoeij et al., 2010), however there are serious time gaps in the optical remote sensing data series. No follow up of ASTER is foreseen other than HySPIRI (Abrams et al., 2013) which will be operational in 2020, possible the sentinel-2 mission (Drusch et al., 2012) or SPOT can fill this niche however that would require substantial alignment of mapping procedures. In terms of hyperspectral data, airborne instruments will be available for surveys but are no option for monitoring. The present, HYPERION on the EO-1 (Pearlman et al., 2003), and planned, EnMAP (Stuffler et al., 2007), spaceborne hyperspectral instruments cannot ensure high enough revisits to enable long term monitoring of geothermal sites. The present literature under exploits the possibility that remote sensing offers in monitoring geothermal systems. This would be of interest as it could link geothermal systems to climate change. In 1993 (Sturchio et al., 1993), however, it was proposed that surface-water hydrology in combination with climate variations influence the evolution of individual caldera-hosted geothermal systems, however given the state of remote sensing in these days this assumption could not be fully tested. The hypothesis based on age dating of hydrothermal deposits suggested that elevated water table in combination with more water available from (extreme) rain events (during more humid climate condition) resulted in greater transfer of heat from deep heat sources to the surface. Analysis of long time series of remote sensing data over selected geothermal areas in various geodynamic settings could form the basis of accepting or rejecting this hypothesis at least over decades of time spans.

- do surface manifestations link to subsurface features?

Fluid pathways to the surface tend to be fault controlled and fault planes often are curved thus their surface manifestation cannot be directly linked to their subsurface trajectory. In addition, there are several examples of geothermal systems where impermeable cap rock blankets the system thus leaving no noticeable anomalies at the surface. This implies that geologic interpretation of remote sensing products in particular coupling the surface manifestations to the 3D subsurface geology is essential. Likewise, the remote sensing community focuses on surface temperature and heat flux modeling whilst there is also ample literature on subsurface temperature models in various parts of the world (Bonte et al., 2012) based on thermo-mechanical models of the lithosphere and crust (Cloetingh et al., 2010; Tedla et al., 2011). Although the scale and resolution of current satellite gravity observations with GRACE/GOCE and resulting crustal models is too coarse to directly relate them to geothermal systems there is a potential to better understand crustal dynamics and density fluxes that drive the geothermal systems. A good example on the Parana basin in Brazil though directed toward a basin study for petroleum exploration has been recently published (Mariani et al., 2013). Although there is a scale and resolution difference at a continental scale it would be worthwhile to combine these results or start comparative analyses.

- how to bridge the divide between academia and industry?

Geologic remote sensing products have found their way to the value-adding industry: the mining industry and to a lesser extent the oil and gas industry. However the recently published 'geothermal handbook' (Gehringer and Loksha, 2012) only mentions satellite observations once under the heading of a 'preliminary survey', but no mention of the use of remote sensing is made in the exploration stages of developing a geothermal field. The geologic remote sensing community has a bias to publishing results in the remote sensing journals rather than in the geosciences journals. It is evident that a further alignment with industry is essential for the uptake of remote sensing products in practice.

Conclusions

Given that geothermal systems associated with high enthalpy volcanic settings often are in arid regions or due to the nature of the underlying volcanic processes show a high degree of exposed rock outcrop are ideal study sites for remote sensing applications. The number of geothermal fields studied with remote sensing worldwide is limited with an emphasis on systems in the US. There seem no integrated studies combining surface information from remote sensing with subsurface data and ancillary data sets. Exploration of geothermal areas traditionally relies on geophysical prospecting in combination with reservoir modeling. Good case studies would help in show casing the added value of earth observation data in this context. A number of studies have centered on the use of multispectral remote sensing (in particular using ASTER) to do regional reconnaissance studies with the aim to highlight areas of potential for geothermal exploration. The combination of VNIR-SWIR bands, to map surface geology, and TIR bands, to map surface temperature makes ASTER an ideal instrument for that. Several papers have been published on heat flux measurements with thermal infrared remote sensing data sets and few studies have looked into long term monitoring of geothermal systems with MODIS to get a better understanding of the underlying processing governing these systems and the features in space and time. A wealth of papers focuses on the use of hyperspectral data to map surface alteration mineralogy of geothermal sites and some papers investigated long-term subsidence and uplift of geothermal areas related to exploitation of reservoirs. There seems scope for more studies in particular also combining observations on various systems in different geologic regimes (rift related, subduction related, high enthalpy, steam heated etc.) to better link the observations to the underlying drivers of the systems. There are at present no environmental impact studies related to geothermal exploration although this is an area where earth observation and geospatial modeling could play an influential role.

Acknowledgement

In large this review is based on peer reviewed (ISI) journal papers for the sake of accessibility to the readers of our review. We apologize to those authors whose papers have not been included. This paper resulted from a number of (key note) presentations that we have given at various conferences. Thanks are due to Carlos de Souza Filho (UNICAMP), Benoit Rivard (University of Alberta), Jan Diederik van Wees (TNO, UU), Guus Willemsen (IF Technology), David Bruhn (GFZ), Ninik Suryantini (ITB), Anupma Prakash (University of Fairbanks) and Tom Cudahy (CSIRO). We are grateful to Transmark Renewables for their support to the project. We are grateful to the reviewers for valuable comments that improved our manuscript.

References

Abrams, M., Pieri, D., Realmuto, V., Wright, R., 2013. Using EO-1 Hyperion Data as HysplRI Preparatory Data Sets for Volcanology Applied to Mt Etna, Italy. IEEE J. Sel. Top. Appl. Earth Observ. Remote Sens. 6 (2), 375–385.

Acar, H.I., 2003. A review of geothermal energy in Turkey. Energy Sour. 25 (11), 1083–1088.

Alzwar, M., 1986. Geothermal-energy potential related to active volcanism in Indonesia. Geothermics 15 (5–6), 601–607.

Arnorsson, S., Bjarnason, J.O., Giroud, N., Gunnarsson, I., Stefansson, A., 2006. Sampling and analysis of geothermal fluids. Geofluids 6 (3), 203–216.

Bahadori, A., Zendehboudi, S., Zahedi, G., 2013. A review of geothermal energy resources in Australia: current status and prospects. Renew. Sustain. Energ. Rev. 21, 29–34.
Bailey, J.E., Self, S., Wooller, L.K., Mouginis-Mark, P.J., 2007. Discrimination of fluvial and eolian features on large ignimbrite sheets around La Pacana Caldera, Chile, using Landsat and SRTM-derived DEM. Remote Sens. Environ. 108 (1), 24–41.
Barbier, E., 2002. Geothermal energy technology and current status: an overview. Renew. Sustain. Energ. Rev. 6 (1–2), 3–65.
Bateson, L., Vellico, M., Beaubien, S.E., Pearce, J.M., Annunziatellis, A., Ciotoli, G., Coren, F., Lombardi, S., Marsh, S., 2008. The application of remote-sensing techniques to monitor CO_2-storage sites for surface leakage: method development and testing at Latera (Italy) where naturally produced CO_2 is leaking to the atmosphere. Int. J. Greenhouse Gas Control 2 (3), 388–400.
Battaglia, S., 2004. Variations in the chemical composition of illite from five geothermal fields: a possible geothermometer. Clay Miner. 39 (4), 501–510.
Bedini, E., van der Meer, F., van Ruitenbeek, F., 2009. Use of HyMap imaging spectrometer data to map mineralogy in the Rodalquilar caldera, southeast Spain. Int. J. Remote Sens. 30 (2), 327–348.
Bektas, O., Ravat, D., Bueyueksarac, A., Bilim, F., Ates, A., 2007. Regional geothermal characterisation of East Anatolia from aeromagnetic, heat flow and gravity data. Pure Appl. Geophys. 164 (5), 975–998.
Berhane, D., Mosusu, N., 1997. A review of the geothermal resources of Papua New Guinea, Gem 97 Png. In: Geology Exploration and Mining Conference, Proceedings, pp. 15–27.
Bertani, R., 2005. World geothermal power generation in the period 2001–2005. Geothermics 34 (6), 651–690.
Bertani, R., 2012. Geothermal power generation in the world 2005–2010 update report. Geothermics 41, 1–29.
Bonte, D., van Wees, J.D., Verweij, J.M., 2012. Subsurface temperature of the onshore Netherlands: new temperature dataset and modelling. Netherlands J. Geosci. – Geologie En Mijnbouw 91 (4), 491–515.
Bonte, M., van Breukelen, B.M., Stuyfzand, P.J., 2013. Temperature-induced impacts on groundwater quality and arsenic mobility in anoxic aquifer sediments used for both drinking water and shallow geothermal energy production. Water Res. 47 (14), 5088–5100.
Boothroyd, I.K.G., 2009. Ecological characteristics and management of geothermal systems of the Taupo Volcanic Zone, New Zealand. Geothermics 38 (1), 200–209.
Burns, B., 1997. Vegetation change along a geothermal stress gradient at the Te Kopia steamfield. J. R. Soc. N.Z. 27 (2), 279–294.
Carlino, S., Somma, R., Troise, C., De Natale, G., 2012. The geothermal exploration of Campanian volcanoes: Historical review and future development. Renew. Sustain. Energ. Rev. 16 (1), 1004–1030.
Carnec, C., Fabriol, H., 1999. Monitoring and modeling land subsidence at the Cerro Prieto geothermal field, Baja California, Mexico, using SAR interferometry. Geophys. Res. Lett. 26 (9), 1211–1214.
Carranza, E.J.M., van Ruitenbeek, F.J.A., Hecker, C., van der Meijde, M., van der Meer, F.D., 2008a. Knowledge-guided data-driven evidential belief modeling of mineral prospectivity in Cabo de Gata, SE Spain. Int. J. Appl. Earth Observ. Geoinform. 10 (3), 374–387.
Carranza, E.J.M., Wibowo, H., Barritt, S.D., Sumintadireja, P., 2008b. Spatial data analysis and integration for regional-scale geothermal potential mapping, West Java, Indonesia. Geothermics 37 (3), 267–299.
Clark, R.N., Swayze, G.A., Livo, K.E., Kokaly, R.F., Sutley, S.J., Dalton, J.B., McDougal, R.R., Gent, C.A., 2003. Imaging spectroscopy: earth and planetary remote sensing with the USGS Tetracorder and expert systems. J. Geophys. Res. 108 (E12.).
Cloetingh, S., van Wees, J.D., Ziegler, P.A., Lenkey, L., Beekman, F., Tesauro, M., Forster, A., Norden, B., Kaban, M., Hardebol, N., Bonte, D., Genter, A., Guillou-Frottier, L., Ter Voorde, M., Sokoutis, D., Willingshofer, E., Cornu, T., Worum, G., 2010. Lithosphere tectonics and thermo-mechanical properties: an integrated modelling approach for Enhanced Geothermal Systems exploration in Europe. Earth Sci. Rev. 102 (3–4), 159–206.
Coolbaugh, M.E., Zehner, R.E., Raines, G.L., Oppliger, G.L., Kreemer, C., 2005. Regional prediction of geothermal systems in the Great Basin, USA using weights of evidence and logistic regression in a geographic information system (GIS). GIS and Spatial Analysis 1–2, 505–510.
Coolbaugh, M.F., Kratt, C., Fallacaro, A., Calvin, W.M., Taranik, J.V., 2007. Detection of geothermal anomalies using Advanced Spaceborne Thermal Emission and Reflection Radiometer (ASTER) thermal infrared images at Bradys Hot Springs, Nevada, USA. Remote Sens. Environ. 106 (3), 350–359.
Crosta, A.P., De Souza, C.R., Azevedo, F., Brodie, C., 2003. Targeting key alteration minerals in epithermal deposits in Patagonia, Argentina, using ASTER imagery and principal component analysis. Int. J. Remote Sens. 24 (21), 4233–4240.
Decaritat, P., Hutcheon, I., Walshe, J.L., 1993. Chlorite geothermometry – a review. Clays Clay Miner. 41 (2), 219–239.
Deroin, J.P., Cochrane, G.R., Mongillo, M.A., Browne, P.R.L., 1995. Methods of remote-sensing in geothermal regions – the geodynamic setting of the Taupo volcanic zone (north-island, New-Zealand). Int. J. Remote Sens. 16 (9), 1663–1677.
Drusch, M., Del Bello, U., Carlier, S., Colin, O., Fernandez, V., Gascon, F., Hoersch, B., Isola, C., Laberinti, P., Martimort, P., Meygret, A., Spoto, F., Sy, O., Marchese, F., Bargellini, P., 2012. Sentinel-2: ESA's Optical High-Resolution Mission for GMES Operational Services. Remote Sens. Environ. 120, 25–36.
Eneva, M., Coolbaugh, M., 2009. Importance of elevation and temperature inversions for the interpretation of thermal infrared satellite images used in geothermal exploration. In: Proceedings Geothermal Resources Council Transactions, vol. 33, pp. 415–418.
Fahselt, D., 1995. Growth form and reproductive character of lichens near active fumaroles in Japan. Symbiosis 18 (3), 211–231.
Fialko, Y., Simons, M., 2000. Deformation and seismicity in the Coso geothermal area, Inyo County, California: observations and modeling using satellite radar interferometry. J. Geophys. Res. 105 (B9), 21781–21793.
Fournier, R.O., White, D.E., 1973. Review of geochemical techniques in geothermal exploration. Geophysics 38 (1), p. 172-&.
Fridleifsson, I.B., 2001. Geothermal energy for the benefit of the people. Renew. Sustain. Energy Rev. 5 (3), 299–312.
Gardeweg, M., Ramírez, C., 1987. La Pacana caldera and the Atana Ignimbrite – a major ash-flow and resurgent caldera complex in the Andes of northern Chile. Bull. Volcanol. 49 (3), 547–566.
Gehringer, M., Loksha, V., 2012. Geothermal handbook: planning and financing power generation, The World Bank., pp. 149.
Giordano, G., Pinton, A., Cianfarra, P., Baez, W., Chiodi, A., Viramonte, J., Norini, G., Groppelli, G., 2013. Structural control on geothermal circulation in the Cerro Tuzgle-Tocomar geothermal volcanic area (Puna plateau, Argentina). J. Volcanol. Geotherm. Res. 249, 77–94.
Gutierrez, F.J., Lemus, M., Parada, M.A., Benavente, O.M., Aguilera, F.A., 2012. Contribution of ground surface altitude difference to thermal anomaly detection using satellite images: Application to volcanic/geothermal complexes in the Andes of Central Chile. J. Volcanol. Geotherm. Res. 237, 69–80.
Hackwell, J.A., Warren, D.W., Bongiovi, R.P., Hansel, S.J., Hayhurst, T.L., Mabry, D.J., Sivjee, M.G., Skinner, J.W., 1996. LWIR/MWIR imaging hyperspectral sensor for airborne and ground-based remote sensing, Imaging Spectrometry Ii., pp. 102–107.
Hansell, A., Oppenheimer, C., 2004. Health hazards from volcanic gases: a systematic literature review. Arch. Environ. Health 59 (12), 628–639.
Haselwimmer, C., Prakash, A., 2013. Thermal infrared remote sensing of geothermal systems. In: Kuenzer, C., Dech, S. (Eds.), Thermal Infrared Remote Sensing, vol. 17. Spinger, Dordrecht, pp. 453–473.
Haselwimmer, C., Prakash, A., Holdmann, G., 2013. Quantifying the heat flux and outflow rate of hot springs using airborne thermal imagery: case study from Pilgrim Hot Springs, Alaska. Remote Sens. Environ. 136, 37–46.
Hellman, M.J., Ramsey, M.S., 2004. Analysis of hot springs and associated deposits in Yellowstone National Park using ASTER and AVIRIS remote sensing. J. Volcanol. Geotherm. Res. 135 (1–2), 195–219.
Henley, R.W., Ellis, A.J., 1983. Geothermal systems ancient and modern - a geochemical review. Earth Sci. Rev. 19 (1), 1–50.
Hepbasli, A., Ozgener, L., 2004. Development of geothermal energy utilization in Turkey: a review. Renew. Sustain. Energy Rev. 8 (5), 433–460.
Hochstein, M.P., Moore, J.N., 2008. Indonesia: Geothermal prospects and developments – preface. Geothermics 37 (3), 217–219.
Hook, S.J., Myers, J.E.J., Thome, K.J., Fitzgerald, M., Kahle, A.B., 2001. The MODIS/ASTER airborne simulator (MASTER) – a new instrument for earth science studies. Remote Sens. Environ. 76 (1), 93–102.
Huang, W.L., Longo, J.M., Pevear, D.R., 1993. An experimentally derived kinetic-model for smectite-to-illite conversion and its use as a geothermometer. Clays Clay Miner. 41 (2), 162–177.
Hubbard, B.E., Crowley, J.K., Zimbelman, D.R., 2003. Comparative alteration mineral mapping using visible to shortwave infrared (0.4–2.4 mu m) Hyperion, ALI, and ASTER imagery. IEEE Trans. Geosci. Remote Sens. 41 (6), 1401–1410.
Huntington, J.F., 1996. The role of remote sensing in finding hydrothermal mineral deposits on Earth. In: Bock, G.R., Goode, J.A. (Eds.), Evolution of Hydrothermal Ecosystems on Earth, vol. 202, pp. 214–235.
Jonsson, S., Adam, N., Bjornsson, H., 1998. Effects of subglacial geothermal activity observed by satellite radar interferometry. Geophysical Research Letters 25 (7), 1059–1062.
Kaiser, M.F., Ahmed, S., 2013. Optimal thermal water locations along the Gulf of Suez coastal zones, Egypt. Renew. Energy 55, 374–379.
Kay, S.M., Coira, B.L., Caffe, P.J., Chen, C.H., 2010. Regional chemical diversity, crustal and mantle sources and evolution of central Andean Puna plateau ignimbrites. J. Volcanol. Geotherm. Res. 198 (1–2), 81–111.
Kealy, P.S., Hook, S.J., 1993. Separating temperature and emissivity in thermal infrared multispectral scanner data – implications for recovering land-surface temperatures. IEEE Trans. Geosci. Remote Sens. 31 (6), 1155–1164.
Kratt, C., Calvin, W.M., Coolbaugh, M.F., 2010. Mineral mapping in the Pyramid Lake basin: hydrothermal alteration, chemical precipitates and geothermal energy potential. Remote Sens. Environ. 114 (10), 2297–2304.
Krohn, M.D., Kendall, C., Evans, J.R., Fries, T.L., 1993. Relations of ammonium minerals at several hydrothermal systems in the western United-States. J. Volcanol. Geotherm. Res. 56 (4), 401–413.
Kruse, F.A., 2012. Mapping surface mineralogy using imaging spectrometry. Geomorphology 137 (1), 41–56.
Kuria, Z.N., Woldai, T., van der Meer, F.D., Barongo, J.O., 2010. Active fault segments as potential earthquake sources: Inferences from integrated geophysical mapping of the Magadi fault system, southern Kenya Rift. J. African Earth Sci. 57 (4), 345–359.
Lees, J.M., 2007. Seismic tomography of magmatic systems. J. Volcanol. Geotherm. Res. 167 (1–4), 37–56.
Lindsay, J.M., de Silva, S., Trumbull, R., Emmermann, R., Wemmer, K., 2001a. La Pacana caldera, N. Chile: a re-evaluation of the stratigraphy and volcanology of one of the world's largest resurgent calderas. J. Volcanol. Geotherm. Res. 106 (1–2), 145–173.
Lindsay, J.M., Schmitt, A.K., Trumbull, R.B., De Silva, S.L., Siebel, W., Emmermann, R., 2001b. Magmatic evolution of the La Pacana caldera system, Central Andes,

Chile: Compositional variation of two cogenetic, large-volume felsic ignimbrites. J. Petrol. 42 (3), 459–486.
Littlefield, E.F., Calvin, W.M., 2014. Geothermal exploration using imaging spectrometer data over Fish Lake Valley, Nevada. Remote Sens. Environ. 140 (0), 509–518.
Liu, J.K., Yu, M.F., Ueng, S.J., 2003. A structure-controlled model for hot spring exploration in Taiwan by remote sensing. Geosci. J. 7 (4), 323–325.
Lubitz, C., Motagh, M., Wetzel, H.U., Kaufmann, H., 2013. Remarkable Urban Uplift in Staufen im Breisgau, Germany: observations from TerraSAR-X InSAR and Leveling from 2008 to 2011. Remote Sens. 5 (6), 3082–3100.
Lund, J.W., Freeston, D.H., Boyd, T.L., 2005. Direct application of geothermal energy: 2005 Worldwide review. Geothermics 34 (6), 691–727.
Majer, E.L., Baria, R., Stark, M., Oates, S., Bommer, J., Smith, B., Asanuma, H., 2007. Induced seismicity associated with enhanced geothermal systems. Geothermics 36 (3), 185–222.
Mariani, P., Braitenberg, C., Ussami, N., 2013. Explaining the thick crust in Parana basin, Brazil, with satellite GOCE gravity observations. J. South American Earth Sci. 45, 209–223.
Mars, J.C., Rowan, L.C., 2006. Regional mapping of phyllic- and argillic-altered rocks in the Zagros magmatic arc, Iran, using Advanced Spaceborne Thermal Emission and Reflection Radiometer (ASTER) data and logical operator algorithms. Geosphere 2 (3), 161–186.
Mars, J.C., Rowan, L.C., 2010. Spectral assessment of new ASTER SWIR surface reflectance data products for spectroscopic mapping of rocks and minerals. Remote Sens. Environ. 114 (9), 2011–2025.
Martini, B.A., Cocks, T.D., Cocks, P.A., Pickles, W.L., IEEE, 2004. Operational airborne hyperspectral remote sensing for global geothermal exploration, Igarss 2004. In: IEEE International Geoscience and Remote Sensing Symposium Proceedings, Vols. 1–7: Science for Society: Exploring and Managing a Changing Planet, pp. 625–626.
Martini, B.A., Silver, E.A., Pickles, W.L., Cocks, P.A., 2003. Hyperspectral mineral mapping in support of geothermal exploration: examples from Long Valley Caldera, CA and Dixie Valley, NV, USA. In: Proceedings Geothermal Resources Council Transactions, vol. 27, pp. 415–418.
Mock, J.E., Tester, J.W., Wright, P.M., 1997. Geothermal energy from the earth: its potential impact as an environmentally sustainable resource. Annu. Rev. Energy Environ. 22, 305–356.
Mongillo, M.A., 1994. Aerial thermal infrared mapping of the Waimangu-Waiotapu geothermal region, New-Zealand. Geothermics 23 (5–6), 511–526.
Nash, G.D., Johnson, G.W., Johnson, S., 2004. Hyperspectral detection of geothermal system-related soil mineralogy anomalies in Dixie Valley, Nevada: a tool for exploration. Geothermics 33 (6), 695–711.
Nash, G.D., Moore, J.N., Sperry, T., 2003. Vegetal-spectral anomaly detection at the Cove Fort-Sulphurdale thermal anomaly, Utah, USA: implications for use in geothermal exploration. Geothermics 32 (2), 109–130.
Noomen, M.F., Skidmore, A.K., 2009. The effects of high soil CO_2 concentrations on leaf reflectance of maize plants. Int. J. Remote Sens. 30 (2), 481–497.
O'Sullivan, M.J., Pruess, K., Lippmann, M.J., 2001. State of the art of geothermal reservoir simulation. Geothermics 30 (4), 395–429.
Peacock, J.R., Thiel, S., Heinson, G.S., Reid, P., 2013. Time-lapse magnetotelluric monitoring of an enhanced geothermal system. Geophysics 78 (3), B121–B130.
Pearlman, J.S., Barry, P.S., Segal, C.C., Shepanski, J., Beiso, D., Carman, S.L., 2003. Hyperion, a space-based imaging spectrometer. IEEE Trans. Geosci. Remote Sens. 41 (6), 1160–1173.
Pieri, D., Abrams, M., 2004. ASTER watches the world's volcanoes: a new paradigm for volcanological observations from orbit. J. Volcanol. Geotherm. Res. 135 (1–2), 13–28.
Qin, Q.M., Zhang, N., Nan, P., Chai, L.L., 2011. Geothermal area detection using Landsat ETM plus thermal infrared data and its mechanistic analysis-A case study in Tengchong, China. Int. J. Appl. Earth Observ. Geoinform. 13 (4), 552–559.
Ramsey, M.S., Harris, A.J.L., 2013. Volcanology 2020: how will thermal remote sensing of volcanic surface activity evolve over the next decade? J. Volcanol. Geotherm. Res. 249, 217–233.
Reath, K.A., Ramsey, M.S., 2013. Exploration of geothermal systems using hyperspectral thermal infrared remote sensing. J. Volcanol. Geotherm. Res. 265, 27–38.
Rowan, L.C., Hook, S.J., Abrams, M.J., Mars, J.C., 2003. Mapping hydrothermally altered rocks at Cuprite, Nevada, using the advanced Spaceborne Thermal Emission and Reflection Radiometer (ASTER), a new satellite-imaging system. Econ. Geol. 98 (5), 1019–1027.
Sass, I., Burbaum, U., 2010. Damage to the historic town of Staufen (Germany) caused by geothermal drillings through anhydrite-bearing formations. Acta Carsologica 39 (2), 233–245.
Savage, S.L., Lawrence, R.L., Custer, S.G., Jewett, J.T., Powell, S.L., Shaw, J.A., 2010. Review of alternative methods for estimating terrestrial emittance and geothermal heat flux for Yellowstone national park using landsat imagery. Gisci. Remote Sens. 47 (4), 460–479.
Schnurr, W.B.W., Trumbull, R.B., Clavero, J., Hahne, K., Siebel, W., Gardeweg, M., 2007. Twenty-five million years of silicic volcanism in the southern central volcanic zone of the Andes: geochemistry and magma genesis of ignimbrites from 25 to 27 degrees S, 67–72 degrees W. J. Volcanol. Geotherm. Res. 166 (1), 17–46.
Sekioka, M., 1985. Geothermal observations by use of a helicopter-borne remote-sensing system. Remote Sens. Environ. 18 (2), 193–203.
Shoham, Y., 1978. Magnetotelluric geophysical exploration method – review. AAPG Bull.-Am. Assoc. Petrol. Geol. 62 (11), 2362.
Snoeij, P., Attema, E., Davidson, M., Duesmann, B., Floury, N., Levrini, G., Rommen, B., Rosich, B., 2010. Sentinel-l radar mission: status and performance. IEEE Aerospace Electron. Syst. Mag. 25 (8), 32–39.
Stuffler, T., Kaufmann, C., Hofer, S., Forster, K.P., Schreier, G., Mueller, A., Eckardt, A., Bach, H., Penne, B., Benz, U., Haydn, R., 2007. The EnMAP hyperspectral imager – an advanced optical payload for future applications in Earth observation programmes. Acta Astronautica 61 (1–6), 115–120.
Sturchio, N.C., Dunkley, P.N., Smith, M., 1993. Climate-driven variations in geothermal activity in the northern Kenya rift valley. Nature 362 (6417), 233–234.
Tank, V., Pfanz, H., Kick, H., 2008. New remote sensing techniques for the detection and quantification of earth surface CO_2 degassing. J. Volcanol. Geotherm. Res. 177 (2), 515–524.
Tedla, G.E., van der Meijde, M., Nyblade, A.A., van der Meer, F.D., 2011. A crustal thickness map of Africa derived from a global gravity field model using Euler deconvolution. Geophys. J. Int. 187 (1), 1–9.
Tester, J.W., Anderson, B.J., Batchelor, A.S., Blackwell, D.D., DiPippo, R., Drake, E.M., Garnish, J., Livesay, B., Moore, M.C., Nichols, K., Petty, S., Toksoz, M.N., Veatch, R.W., Baria, R., Augustine, C., Murphy, E., Negraru, P., Richards, M., 2007. Impact of enhanced geothermal systems on US energy supply in the twenty-first century. Phil. Trans. R. Soc. 365 (1853), 1057–1094.
Tole, M.P., 1996. Geothermal energy research in Kenya: a review. J. African Earth Sci. 23 (4), 565–575.
Ulusoy, I., Labazuy, P., Aydar, E., 2012. STcorr: An IDL code for image based normalization of lapse rate and illumination effects on nighttime TIR imagery. Comput. Geosci. 43, 63–72.
van der Meer, F.D., van der Werff, H.M.A., van Ruitenbeek, F.J.A., Hecker, C.A., Bakker, W.H., Noomen, M.F., van der Meijde, M., Carranza, E.J.M., de Smeth, J.B., Woldai, T., 2012. Multi- and hyperspectral geologic remote sensing: a review. Int. J. Appl. Earth Observ. Geoinform. 14 (1), 112–128.
van Ruitenbeek, F.J.A., Cudahy, T., Hale, M., van der Meer, F.D., 2005. Tracing fluid pathways in fossil hydrothermal systems with near-infrared spectroscopy. Geology 33 (7), 597–600.
Vaughan, R.G., Hook, S.J., Calvin, W.M., Taranik, J.V., 2005. Surface mineral mapping at Steamboat Springs, Nevada, USA, with multi-wavelength thermal infrared images. Remote Sens. Environ. 99 (1–2), 140–158.
Vaughan, R.G., Keszthelyi, L.P., Davies, A.G., Schneider, D.J., Jaworowski, C., Heasler, H., 2010. Exploring the limits of identifying sub-pixel thermal features using ASTER TIR data. J. Volcanol. Geotherm. Res. 189 (3–4), 225–237.
Vaughan, R.G., Keszthelyi, L.P., Lowenstern, J.B., Jaworowski, C., Heasler, H., 2012. Use of ASTER and MODIS thermal infrared data to quantify heat flow and hydrothermal change at Yellowstone National Park. J. Volcanol. Geotherm. Res. 233, 72–89.
Verma, S.P., Santoyo, E., 1997. New improved equations for Na/K, Na/Li and SiO_2 geothermometers by outlier detection and rejection. J. Volcanol. Geotherm. Res. 79 (1–2), 9–23.
Vodnik, D., Kastelec, D., Pfanz, H., Macek, I., Turk, B., 2006. Small-scale spatial variation in soil CO_2 concentration in a natural carbon dioxide spring and some related plant responses. Geoderma 133 (3–4), 309–319.
Watson, F.G.R., Lockwood, R.E., Newman, W.B., Anderson, T.N., Garrott, R.A., 2008. Development and comparison of Landsat radiometric and snowpack model inversion techniques for estimating geothermal heat flux. Remote Sens. Environ. 112 (2), 471–481.
Young, S.J., Johnson, B.R., Hackwell, J.A., 2002. An in-scene method for atmospheric compensation of thermal hyperspectral data. Journal of Geophysical Research-Atmospheres 107 (D24).
Zohdy, A.A.R., Anderson, L.A., Muffler, L.J.P., 1973. Resistivity, self-potential, and induced-polarization surveys of a vapor-dominated geothermal system. Geophysics 38 (6), 1130–1144.